Fluorescence and Fluorescence-Excitation Spectra of Benzo[*f*]quinoline during the Sol–Gel–Xerogel Transitions of Mixed Silicon–Aluminum Alkoxide Systems

Toshiaki MABUCHI and Tsuneo FUJII*

Department of Chemistry and Material Engineering, Faculty of Engineering, Shinshu University, Wakasato, Nagano 380

(Received February 12, 1993)

The fluorescence and fluorescence-excitation spectra of doped benzo[*f*]quinoline (BQ) during the sol–gel–xerogel transitions of two reaction systems of mixed alkoxides that were catalyzed by HCl and NaOH (or NH_3) have been observed as a function of time. The mixed alkoxides were comprised of tetraethyl orthosilicate (TEOS) and diisobutoxyaluminum triethyl silicate (SAE) (Si : Al=10 : 0 and 9 : 1). During the reaction, it was found that BQ forms three different fluorescent species, neutral, protonated, and an ion pair. The neutral form was seen in the first stage of the reaction and emitted a structured fluorescence. The protonated form appeared in the next reaction stage and it gave a broad and structureless band with a peak around 440 nm. The ion-pair form, produced from BQ and an –OH group of –O–Si–O– and/or –O–Si–O–Al–O– networks, appeared in the last stage of the reaction and its fluorescence peak was located at around 400 nm. The ion pair could not be detected in solutions, but it was found in the xerogel state. The appearance and disappearance of the three species of BQ reflect the condition of microenvironment around the doped BQ during the sol–gel reaction of the TEOS and TEOS+SAE systems. Therefore, the measurements of the fluorescence spectra of BQ are useful for the photophysical investigation on the sol–gel–xerogel transitions of systems containing metal alkoxides such as TEOS and TEOS+SAE.

An active direction for new material chemistry is a low temperature method of synthesizing inorganic glasses by the sol–gel process.[1—4] The advantages of room-temperature incorporation of functional dyes into the glass network through the sol–gel process suggest many possibilities for new photonic materials.[5—8] The sol–gel process has a number of distinct advantages, for example, it enables one to prepare glass matrices at a low temperature that have a high purity; it is also adaptable to producing bulk pieces as well as film and fibers, etc. However, the process also has a number of disadvantages from the standpoint of preparation of inorganic materials. Some of the disadvantages, such as the large shrinkage associated with the gelation process and drying of the gels, etc. Mackenzie[9] has pointed out that the most serious problem in any application of the sol–gel process is the lack of the scientific understanding of many complexities associated with the process at present.

In previous papers we showed that the observation of the fluorescence spectra of 1-naphthol, a proton donor, is a useful photophysical probe on a molecular level for studying the sol–gel process using tetraethyl orthosilicate (TEOS)[10] and mixed alkoxides comprising TEOS and diisobutoxyaluminum triethyl silicate (SAE).[11,12] The results showed that the sol–gel reaction for system including TEOS and SAE proceeded more rapidly than that for systems including TEOS. Since silica–alumina and zeolites are well-known and important acid catalysts, the results have been discussed in connection with the effect of Si+Al composition, structural change, and acidity of the prepared gels.[10—13]

Here we report the fluorescence and fluorescence-excitation spectra of benzo[*f*]quinoline (BQ, a proton acceptor) during the sol–gel–xerogel transitions of mixed alkoxides comprising TEOS and SAE (Si : Al=10 : 0 and 9 : 1, abbreviated systems A and B, respectively). The incorporated molecules are also important as photophysical probes for elucidating the structural evolution of glass as it evolves from sol to gel to xerogel during the sol–gel process. BQ is a weak base in its ground state with the pK_as of their conjugated acids being 5.1.[14—17] The pK_a^* value of its lowest excited singlet state has been reported to be around 11 for BQ.[14—17] These values indicate that BQ is relatively stronger base in its lowest excited singlet state. Therefore, BQ is a suitable probe for photochemical and photophysical processes that result from the interaction between BQ and its surrounding proton-donating molecules and/or matrix which may be produced during the sol–gel reaction. Based on the experimental findings, we discuss the relationship of fluorescence spectra and species of BQ in the ground and excited states. The structural evolution around doped BQ during sol–gel–xerogel transitions is also discussed.

Experimental

Benzo[*f*]quinoline (Wako Pure Chemical Industries, Inc., JIS S grade), hydrochloric acid (Wako, JIS S), sodium hydroxide (Wako, JIS S), ammonia (Wako, JIS S, 28%), ethanol (Wako, JIS S or S. S. G. grade), cyclohexane (Wako, Luminasol grade), fluorosulfuric acid (FSO_3H, Wako), TEOS (Wako), and SAE (Dynamit Nobel) were used without further purification. Water was deionized and distilled.

The starting solutions of system A contained 11.4 mL of BQ in ethanol (1.69×10^{-4} M (1 M=1 mol dm^{-3})), 10 mL of TEOS, and 3.7 mL of 1×10^{-4} M HCl (A-HCl) or 1×10^{-4} M NaOH (A-NaOH) as a catalyst. Whereas, the starting solutions of system B consisted of 10.0 mL of BQ in ethanol (9.45×10^{-5} M), 10 mL of TEOS+SAE mixed alkoxide (Si : Al=9 : 1), and 0.1 mL of 0.2 M HCl (B-HCl) of 14.7

M NH_3 (B-NH_3) as a catalyst. Syneresis was observed in system A after it was catalyzed by NH_3 making it impossible to observe reasonable emission spectra in the middle stage of the sol–gel reaction; therefore the results were not reported here. The mixtures were thoroughly stirred and then poured into individual plastic cells. They were covered by a thin polymer film with five pinholes and allowed to undergo the sol–gel–xerogel reactions at room temperature under dark (or weak light) condition. The concentrations for the fluorescence and fluorescence-excitation measurements in solution were of the order of 10^{-5} M. The emission spectra were observed using a Shimadzu RF-5000 fluorescence spectrophotometer with the surface emission method. The data were transferred to an NEC PC-9801 microcomputer for processing.

Results

Fluorescence and Fluorescence- Excitation Spectra of BQ in Typical Solvents. The fluorescence spectra of BQ in cyclohexane, ethanol, 0.2 M NaOH, H_2O, and 1.7 M FSO_3H are shown in Fig. 1. Except for H_2O, none of the spectra exhibited excitation wavelength dependence. The spectrum observed in cyclohexane shows fine vibrational structures and is located at the shorter wavelength (higher energy) side than the others. Although the peak location exhibits a small red shift compared to that observed in cyclohexane, the spectrum observed in ethanol essentially maintains the spectral features observed in cyclohexane. The spectrum observed in 0.2 M NaOH showed less structured fluorescence; however, its spectral features were similar to those observed in ethanol, even though individual vibrational bands became more diffuse. In addition to the structured fluorescence band, BQ shows a broad and structureless fluorescence band in H_2O and 1.7 M FSO_3H. Although the results are not shown here, the spectrum excited at 360 nm in H_2O showed only a broad band. The peak wavelength of the broad fluorescence was found at 440 nm in 1.7 M FSO_3H. These spectral features of BQ are essentially the same as reported by Marzzacco et al.[17] Hereafter we abbreviate the structured fluorescence spectrum typically observed in cyclohexane and ethanol to FN and the broad fluorescence spectrum typically observed in 1.7 M FSO_3H to FP.

The fluorescence-excitation spectra of BQ in cyclohexane, ethanol, 0.2 M NaOH, H_2O, and 1.7 M FSO_3H are shown in Fig. 2. Except for H_2O, none of the spectra exhibited excitation wavelength dependence. They consist of two characteristic spectra: One is observed in cyclohexane, and the other is observed in 1.7 M FSO_3H. Although the vibrational structures were somewhat broad, similar fluorescence-excitation spectra were observed in ethanol and 0.2 M NaOH. On the other hand, the spectrum observed in H_2O and 1.7 M FSO_3H shows a broad and structureless band with its peak wavelength located at 360 nm. It should be noted

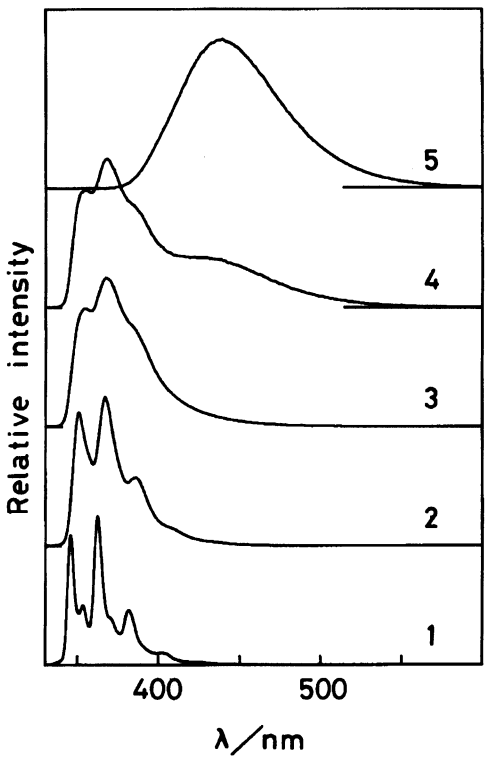

Fig. 1. Fluorescence spectra of BQ in cyclohexane (1), ethanol (2), 0.2 M NaOH (3), H_2O (4), and 1.7 M FSO_3H (5). Excitation wavelength: 320 nm.

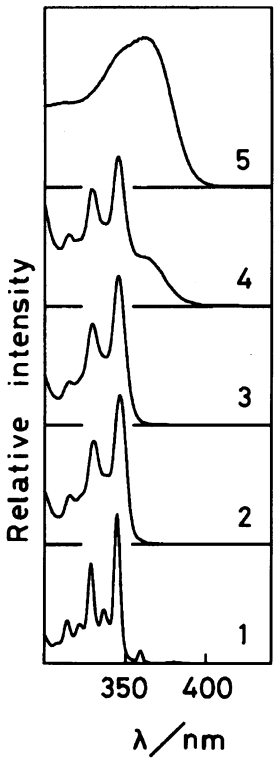

Fig. 2. Fluorescence-excitation spectra of BQ in cyclohexane (1), ethanol (2), 0.2 M NaOH (3), H_2O (4), and 1.7 M FSO_3H (5). Monitored at 400 nm for (1), (2), and (3), and 450 nm for (4) and (5).

that the relative intensity of the broad band monitored at 500 nm in H_2O increased.

Fluorescence and Fluorescence- Excitation Spectra of BQ during the Sol to Gel to Xerogel Transitions. Figure 3 shows the fluorescence spectra of BQ during the sol–gel–xerogel transitions of system A-HCl as a function of time. Just after mixing, the fluorescence spectrum shows fine vibrational structures and the peak wavelengths are located at 351, 367, and 386 nm. This spectrum essentially corresponds to that observed in ethanol. It took 142 h for gelation. At the gelation time, the spectrum was comprised of two characteristic spectra: One was the FN and the other the FP. The relative intensity of FP to that of FN increased gradually with a lapse of time. After 542 h, the reaction system having a wet gel state mainly gave the FP emission. The fluorescence intensity of FN compared to that of FP became very weak after 9300 h. It should be noted that FP shifted slightly to blue and that a shoulder (ca. 400 nm) at the blue side of FP appeared in the last stage of the reaction (xerogel state after 2557 h). The observed fluorescence spectrum of BQ in 1.7 M FSO_3H showed a peak at 440 nm (line 5 in Fig. 1); however, the peaks observed during the xerogel transition from the wet gel state were located at 430, 426, and 423 nm after 542, 2557, and 9300 h, respectively.

The fluorescence-excitation spectra of BQ during the sol–gel–xerogel transitions of system A-HCl are shown in Fig. 4 as a function of time. Just after mixing, the spectrum shows fine vibrational structures that peaked at 315, 330, and 346 nm. This spectral feature is similar to that observed in ethanol and 0.2 M NaOH; however, an additional band around 370 nm. The band intensity increased with a lapse of time as shown in Fig. 4. The fluorescence excitation band around 370 nm became the main component after 542 (the wet gel state), 2557, and 9300 h (the xerogel state). The excitation band observed after 9300 h is similar to that observed in 1.7 M FSO_3H in the spectral shape. The band peak in 1.7 M FSO_3H is located at 360 nm. The peaks of fluorescence-excitation spectra for the wet gel–the xerogel transition are located at 370, 370, and 374 nm after 542, 2557, and 9300 h, respectively.

Figure 5 shows the fluorescence spectra of BQ during the sol–gel–xerogel transitions of system A-NaOH as a function of time. The gelation occurred after 91 h. The whole spectral change during the sol–gel reaction is similar to that observed in system A-HCl. FN is the main fluorescent component in the first stage of the reaction. The intensity of FP gradually increased, and the FP band became the main fluorescent component after 542 h. In addition, the blue shift of FP and the

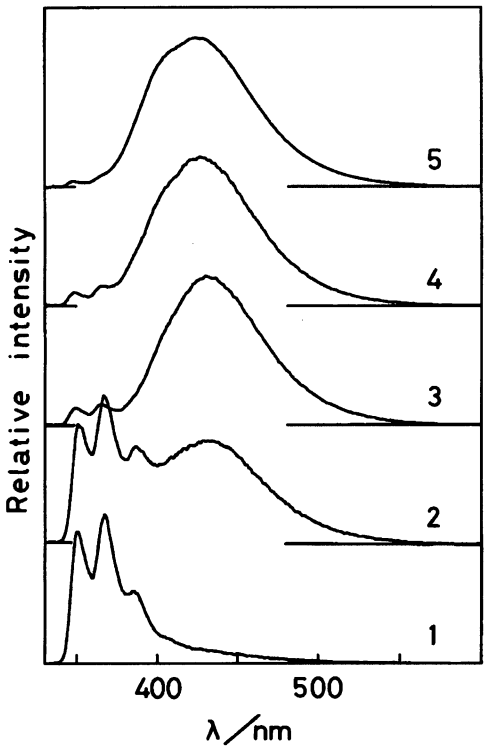

Fig. 3. Fluorescence spectra of BQ in system A-HCl during the sol–gel–xerogel transitions: after 1 h (1), 142 h (2), 542 h (3), 2557 h (4), and 9300 h (5). Excitation wavelength: 320 nm.

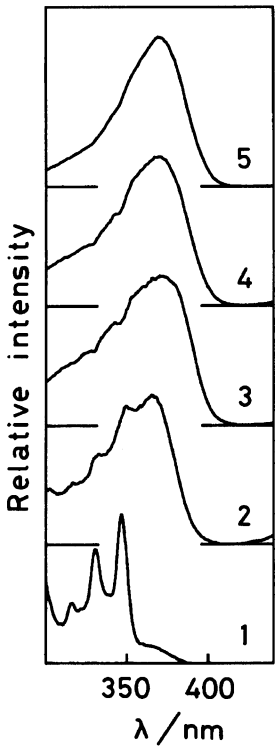

Fig. 4. Fluorescence-excitation spectra of BQ in system A-HCl during the sol–gel–xerogel transitions: after 1 h (1), 142 h (2), 542 h (3), 2557 h (4), and 9300 h (5). Monitored at 400 nm for (1) and (2), and 450 nm for (3), (4), and (5).

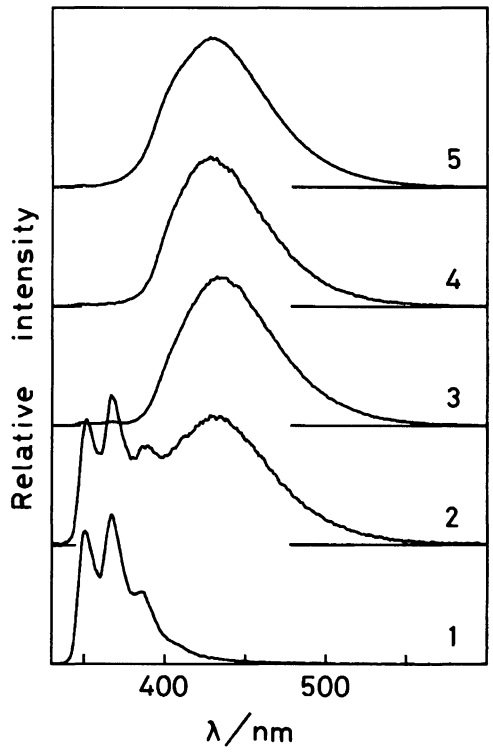

Fig. 5. Fluorescence spectra of BQ in system A-NaOH during the sol–gel–xerogel transitions: after 1 h (1), 91 h (2), 542 h (3), 2557 h (4), and 9300 h (5). Excitation wavelength: 320 nm.

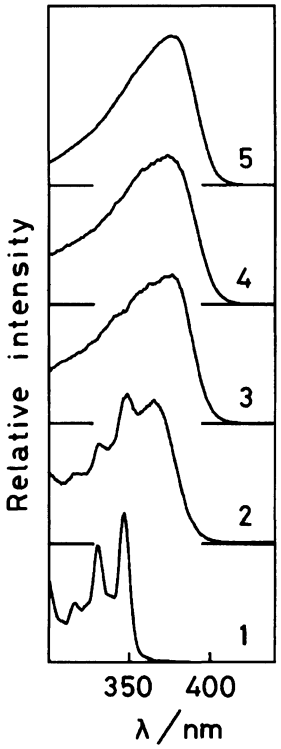

Fig. 6. Fluorescence-excitation spectra of BQ in system A-NaOH during the sol–gel–xerogel transitions: after 1 h (1), 91 h (2), 542 h (3), 2557 h (4), and 9300 h (5). Monitored at 400 nm for (1) and (2), and 450 nm for (3), (4), and (5).

appearance of a shoulder at ca. 400 nm was observed in the xerogel state.

The fluorescence-excitation spectra of BQ during the sol–gel–xerogel transitions of system A-NaOH as a function of time are shown in Fig. 6. The whole spectral features change during the sol–gel reaction is also similar to that observed in the A-HCl reaction system.

Figure 7 shows the fluorescence spectra of BQ during the sol–gel–xerogel transitions of system B-HCl as a function of time. Just after mixing, it is noted that the FP band already became the major band in the first stage of the reaction. The spectrum comprises two characteristic bands, FN and FP. FN shows fine vibrational structures with peak wavelengths located at 351 and 367 nm. The gelation occurred after 80 h. The intensity of FP relative to that of FN increased rapidly as the sol–gel–xerogel reactions progressed. After 5 h, the intensity of FP became the main fluorescence. On the other hand, the fluorescence spectrum observed at the gelation time shifted to blue compared with that observed at 5 h. The fluorescence spectra further shifted to blue after 800 h, and the peak was located at 414 nm. The appearance of a new band (abbreviated to the FI band) around 400 nm resulted in the blue shift. A similar blue shift was also observed in Fig. 3. After 2000 h, in the xerogel state, the peak shifted to red at 423 nm. The new peak at 400 nm was observed after 80 h.

The fluorescence-excitation spectra of BQ during the sol–gel–xerogel transitions of system B-HCl as a function of time are shown in Fig. 8. Just after mixing, the spectrum shows no vibrational peaks and has a broad peak at 365 nm in contrast to systems A. This excitation band is similar to that observed in 1.7 M FSO_3H as shown in Fig. 2 and the xerogel states as shown in Figs. 4 and 6. During the sol–gel reaction, the broad excitation band around 365 nm became broader but retained the main band.

Figure 9 shows the fluorescence spectra of BQ during the sol–gel–xerogel transitions of system B-NH_3 as a function of time. Just after mixing, the fluorescence spectrum shows fine vibrational structures at 351, 367, and 386 nm. This spectrum corresponds to FN as shown in Figs. 1, 3, and 5. The gelation occurred after 134 h. The whole spectral change in the sol–gel reaction is similar to that observed in system B-HCl, except for the appearance of FN after 1 h. FN was the main fluorescent component in the first stage of the reaction. The intensity of FP increased rapidly and after 5 h the FP band became the main fluorescent component. After 134 and 800 h, the peak shifted to blue. After 2000 h, the band peak shifted to red. These blue and red shifts are similar to those observed in system B-HCl as shown in Fig. 7. The peaks are located at 434, 426, 418, and 425 nm after 5, 134, 800, and 2000 h, respectively.

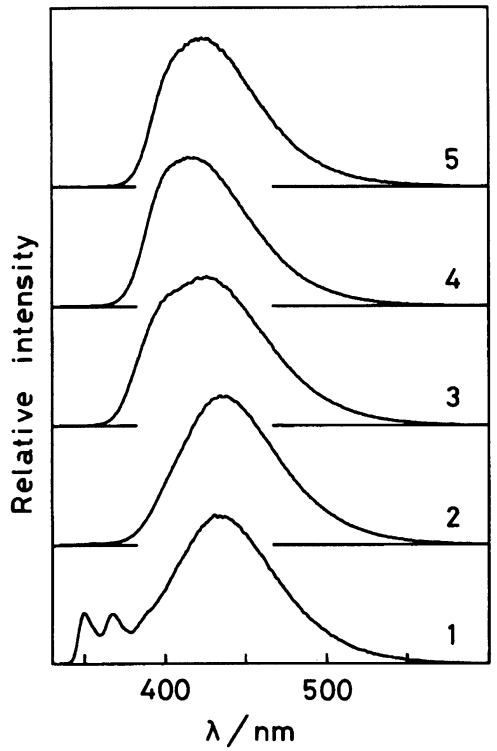

Fig. 7. Fluorescence spectra of BQ in system B-HCl during the sol–gel–xerogel transitions: after 1 h (1), 5 h (2), 80 h (3), 800 h (4), and 2000 h (5). Excitation wavelength: 320 nm.

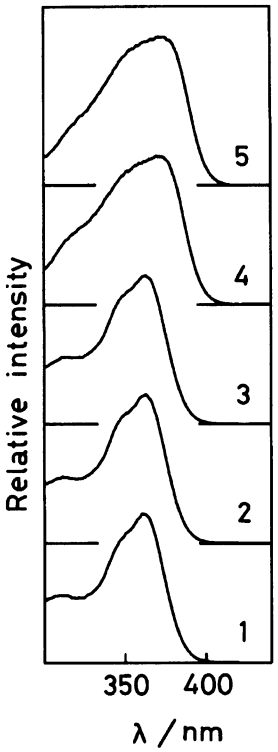

Fig. 8. Fluorescence-excitation spectra of BQ in system B-HCl during the sol–gel–xerogel transitions: after 1 h (1), 5 h (2), 80 h (3), 800 h (4), and 2000 h (5). Monitored at 450 nm.

The fluorescence-excitation spectra of BQ during the sol–gel–xerogel transitions of system B-NH_3 as a function of time are shown in Fig. 10. The whole spectral change during the sol–gel reaction was also similar to that observed in system B-HCl as shown in Fig. 8.

In addition to the results shown in Figs. 3 to 10, we also observed the fluorescence and fluorescence-excitation spectra of BQ at different excitation and emission wavelengths during the sol–gel–xerogel transitions for systems A and B as a function of time. Although the individual fluorescent components appeared in the fluorescence spectra and the individual absorption components in the fluorescence-excitation spectra were different to a certain extent, the overall spectral profile was essentially the same as those presented in Figs. 3, 4, 5, 6, 7, 8, 9, and 10. Figure 11 shows an example of wavelength dependence observed in the fluorescence-excitation spectra of BQ during the sol–gel–xerogel transitions of system A-HCl as a function of the time. Both spectra comprise two components: One has sharp vibrational structures and the other a broad band around 365 nm. It is obvious that the spectra observed at 400 nm show fine vibrational bands more than those observed at 450 nm. This difference corresponds to the different contributions to the fluorescence intensities at 400 and 450 nm from the FI and FP bands, respectively. It is noted that the fluorescence-excitation spectra observed after 9300 h was emission wavelength dependent. This dependence indicates that the molecular species that emit the FI and FP bands are ascribed to the different species in both the ground and excited states.

Discussion

Molecular Species of BQ during the Sol–Gel–Xerogel Transitions. The spectral features observed at the first stage of the sol–gel reaction (lines 1 in Figs. 3, 5, and 9) are very similar to the fluorescence spectrum of BQ in ethanol (line 2 in Fig. 1). The fluorescence-excitation spectrum of BQ in ethanol and those observed at the first stage of the reaction usually have the fine vibrational structures located at ca. 330 and 345 nm. The absorption band at 345 nm in cyclohexane can be assigned to that of the neutral form of BQ. Although the vibrational band both in ethanol and in the first stage of the sol–gel reaction are not so sharp compared to that in cyclohexane, the nature of the ground and excited states of BQ can be regarded as the neutral form of BQ. As a result, FN can be assigned to a fluorescence originated from the neutral form of BQ. The fluorescence-excitation spectra observed in ethanol, 0.2 M NaOH, H_2O, and in the first stage of the sol–gel reaction are somewhat broader than that observed in cyclohexane. This broadness indicates that there is some intermolecular interaction between BQ and the surrounding polar solvents.

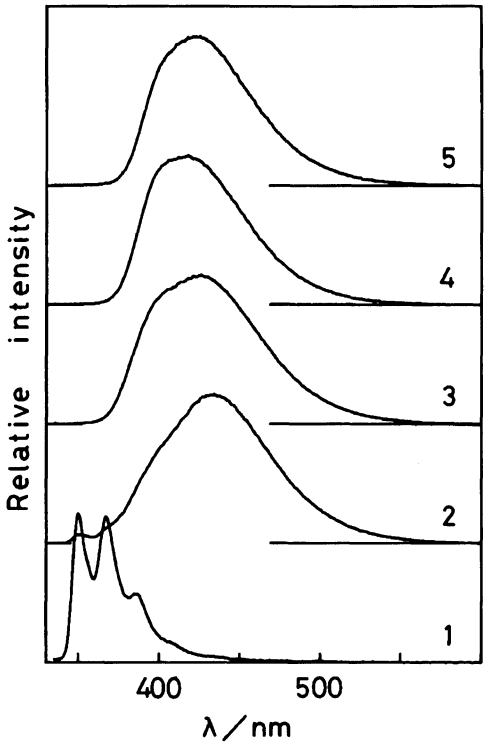

Fig. 9. Fluorescence spectra of BQ in system B-NH_3 during the sol–gel–xerogel transitions: after 1 h (1), 5 h (2), 134 h (3), 800 h (4), and 2000 h (5). Excitation wavelength: 320 nm.

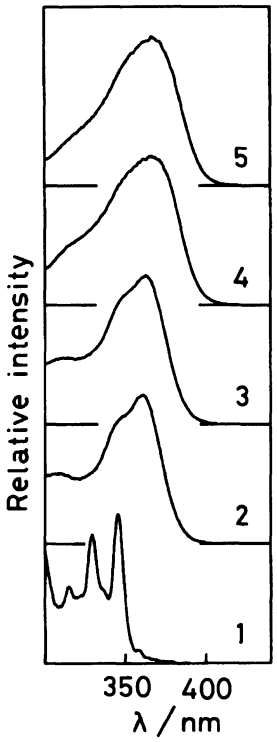

Fig. 10. Fluorescence-excitation spectra of BQ in system B-NH_3 during the sol–gel–xerogel transitions: after 1 h (1), 5 h (2), 134 h (3), 800 h (4), and 2000 h (5). Monitored at 400 nm for (1), and 450 nm for (2), (3), (4), and (5).

BQ acts as a proton acceptor at the nitrogen atom, and FSO_3H is a strong proton donor. The broad and structureless fluorescence band (the FP band) is assigned to originate from the protonated form of BQ, because in its excited singlet state of BQ is a stronger proton acceptor than in its ground state.[17]

Ion pairs are frequently involved as intermediates in organic reactions.[18] Shizuka et al. studied the fluorescence spectra of a hydrogen-bonded system between 1-naphthol and an aliphatic amine in nonpolar rigid matrices at 77 K.[19] The fluorescence spectrum originated from the contact ion-pair state of naphtholate anion with protonated amine excited in the blue side compared to that of the separated one by means of nanosecond time-resolved emission spectroscopy. Recently, we found that some of doped 1-naphthol molecules in the ground state form a contact ion-pair on the surface in cages of the xerogels prepared from TEOS and SAE (Si : Al=94 : 6).[12] In addition to this, the excited-state species having a ground-state ion-pair structure gave the fluorescence originating from both the contact ion pair and an anionic form. This spectral behavior shown for 1-naphthol during the sol–gel–xerogel transitions is similar to the results obtained in the present work.

Based on the above results, we can interpret the ground-state species of BQ observed in the fluorescence and fluorescence-excitation spectra during the sol–gel–xerogel transitions as follows. The broad band around 365 nm in the fluorescence-excitation spectra is concluded to be originated from the ion pair of BQ in the solutions and xerogel state. Upon excitation in solutions, the ion pair is able to relax to a solvent-separated or a protonated form during their fluorescence lifetime and emit FP. The geometrical relaxation is gradually hindered with increasing rigidity around the doped BQ as the sol–gel reaction progresses. As a result, the unrelaxed conformation, namely the contact ion-pair conformer is produced resulting in the emission of FI. A further discussion will be given in the next subsection.

Origin of the Protonated Species During the Sol–Gel–Xerogel Transitions.

The results shown in Figs. 3, 5, 7, and 9 indicate that the molecular species which emits the FP is generated in the reaction systems at the first stage of the sol–gel reaction. The intensity of FP increases significantly during the sol to wet-gel process (e.g. line 2 in Fig. 3) and the wet-gel to xerogel process (e.g. line 3 in Fig. 3). Just after preparation of the reaction system, FP is not clear (e.g. line 1 in Fig. 3) especially for the following systems A-HCl, A-NaOH, and B-NH_3. FP becomes dominant after beginning of the sol–gel reaction in all systems except for system B-HCl.

In the case of $Si(OR)_4$, for example, the whole sol–gel reaction is written as

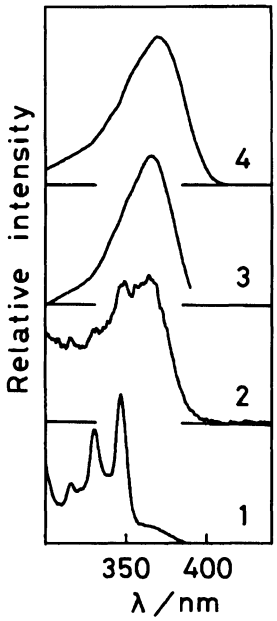

Fig. 11. The fluorescence-excitation spectra of BQ in system A-HCl during the sol–gel–xerogel transitions: after 1 h (1 and 3) and 9300 h (2 and 4). Monitored at 400 nm (1 and 2) and 450 nm (3 and 4).

$$m\mathrm{Si(OR)_4} + 2m\mathrm{H_2O} \rightarrow (\text{–O–Si–O–})_m + 4m\mathrm{ROH} \quad (1)$$

where R is an alkyl group (an ethyl group for TEOS). The sol–gel reaction is characterized by two reaction steps. The first step is the hydrolysis reaction written as

$$\mathrm{Si(OR)_4} + x\mathrm{H_2O} \rightarrow \mathrm{Si(OR)_{4-x}(OH)_x} + x\mathrm{ROH} \quad (2)$$

where x=1—4. The second step of the reaction is stepwise polycondensation by dehydration

$$2\mathrm{Si(OR)_{4-x}(OH)_x} \rightarrow (\mathrm{OH})_{x-1}(\mathrm{OR})_{4-x}\text{–Si} - \mathrm{O}\text{–Si–}(\mathrm{OR})_{4-x}(\mathrm{OH})_{x-1} + \mathrm{H_2O}, \text{ etc.} \quad (3)$$

It was observed that H_2O molecules are consumed by the hydrolysis of silicon alkoxide and simultaneously, alcohol and silanol groups are generated by the reaction Eq. 2, the hydrolysis step. During the reactions, the volatile molecules generated, (alcohol and water molecules) escape from the reaction cell through the pinholes. It is obvious that there is no silanol group in the reaction system before the beginning of the hydrolysis reaction Eq. 2. Therefore, the formation of the silanol groups generated by the reaction step (2) results in the complex formation between the silanol groups and BQ molecules in the ground state, that is, FP originates from the excitation of the ground state complex. The ratio of the intensity of FP to that of FN increases as the sol–gel reaction progresses, reflecting an increase in the silanol group in the reaction systems. Figure 12 illustrates the formation of a molecular form which emits FP with increasing polarity along with hydrolysis of TEOS in the first stage of the sol–gel reaction.

With the progress of the sol–gel reaction, the reactions Eqs. 2 and 3 are nearly completed. Escape of the generated alcohol and water molecules from the reaction system accompanies the completion of the gel structure. Under these circumstances, BQ molecules are placed into small pores of the gel structure and hydrogen bonded with the surrounding silanol groups. The photoexcitation of the BQ complex would relax their geometries under the nonprohibited condition. In fluid solutions, the geometrical relaxation of the hydrogen-bonded complexes is possible resulting in the fluorescence spectrum from the excited protonated state around 440 nm (see Fig. 1). On the other hand, the geometrical relaxation of the hydrogen-bonded BQ complexes would be restricted in the cage of the pore structure of the xerogel. Therefore, the species of the unrelaxed geometrical state, that is the ion pair between BQ and the surface silanol groups, emits fluorescence around 400 nm. Figure 13(a) illustrate a possible geometry of the ion pair formed between BQ and surface silanol groups with gel prepared by systems A in the

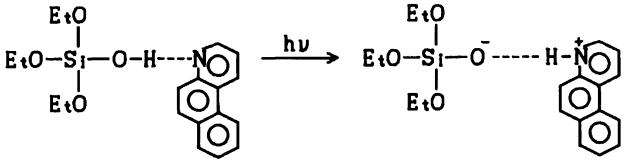

Fig. 12. Formation of the FP species with increasing polarity along hydrolysis of TEOS in the first stage of the sol–gel reaction.

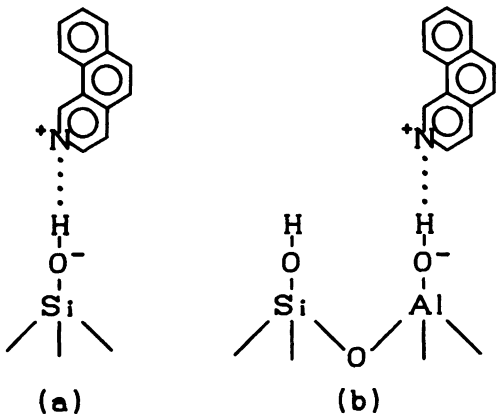

Fig. 13. The geometries of the ion pair formed between BQ and gel surface prepared by (a) systems A and (b) systems B.

xerogel state.

Effect of SAE on the Sol–Gel–Xerogel Transitions. The appearance of the FP component in systems B is faster than in the systems A. The appearance of the FI component in systems A was confirmed at 2557 h, whereas the appearance in system B-HCl was confirmed at 80 h (in system B-NH_3, at 134 h). These differences indicate that the reaction constant of systems B (Si : Al=9 : 1) is faster than that of systems A (Si : Al=10 : 0). The clear appearance of the FI component at relatively shorter time ranges in systems B indicates that the molecular motion during the fluorescence lifetime of the doped BQ in systems B is more restricted than that in systems A. Although the results were not shown here, the gelation time for systems A and B was not largely affected by the change of the amount of catalysts used. The amount of catalyst contained in system A was much larger than that in system B. This different is considered to be not essential factor affecting the difference of the reaction rates between systems A and B. These differences would be caused by the rapid reaction constant of SAE. As a result of the different reaction constants between systems A and B, the properties of the prepared gels, for examples, the pore size, surface area, and acidity, etc. are found to be different between systems A and B. As shown in Figs. 7 and 9, the fluorescence spectra for systems B showed blue shift after 800 h. However, after 2000 h, the spectrum shifted to the red and this fluorescence band is substantially identical with that of systems A. Figure 13(b) illustrate a possible geometry of the ion pair formed between BQ with gel surface prepared by systems B in the wet gel to the xerogel state. It is expected that the geometry in the last stage of systems B may be similar to that shown in Fig. 13(a). Studies of the detailed effect of the sol–gel reaction of mixed alkoxide on the appearance of FN, FP, and FI are in progress.[20]

The authors thank to referees for valuable suggestions. T. F. would like to acknowledge to the financial support from Takamisawa Electric Co., Ltd.

References

1) S. Sakka, "Zoru-geru-hou no Kagaku," Agne-Shofu Sha, Tokyo (1988).
2) "Ultrastructure Processing of Advanced Ceramics," ed by J. D. Mackenzie and D. R. Ulrich, Wiley, New York (1988).
3) C. J. Brinker and G. W. Scherer, "Sol–Gel Science—The Physics and Chemistry of Sol–Gel Processing—," Academic Press, San Diego (1990).
4) L. L. Hench and J. K. West, *Chem. Rev.*, **90**, 33 (1990).
5) D. Avnir, D. Levy, and R. Reisfeld, *J. Phys. Chem.*, **88**, 5956 (1984).
6) D. Avnir, S. Braun, and M. Ottolenghi, *ACS Sympo. Ser.*, **499**, 384 (1992).
7) B. S. Dunn and J. I. Zink, *J. Mater. Chem.*, **1**, 903 (1991); J. I. Zink and B. S. Dunn, *J. Ceram. Soc. Jpn.*, **99**, 878 (1991).
8) T. Fujii, *Hyoumen (Surface)*, **30**, 821 (1992).
9) J. D. Mackenzie, *J. Non-Cryst. Solids*, **100**, 162 (1988).
10) T. Fujii, T. Mabuchi, and I. Mitsui, *Chem. Phys. Lett.*, **168**, 5 (1990).
11) T. Fujii, H. Kitamura, O. Kawauchi, T. Mabuchi, and N. Negishi, *J. Photochem. Photobiol., A: Chem.*, **61**, 365 (1991).
12) T. Fujii, T. Mabuchi, H. Kitamura, O. Kawauchi, N. Negishi, and M. Anpo, *Bull. Chem. Soc. Jpn.*, **65**, 720 (1992).
13) T. Fujii, K. Murayama, N. Negishi, M. Anpo, E. J. Winder, D. R. Neu, and A. B. Ellis, *Bull. Chem. Soc. Jpn.*, **66**, 739 (1993).
14) M. Nakamizo, *Spctrochim. Acta*, **22**, 2039 (1966).
15) A. Grabowska, B. Pakula, and J. Pancir, *Photochem. Photobiol.*, **10**, 415 (1969).
16) E. Vander Donckt, T. Dramaix, K. Nasielski, and C. Vogels, *Trans. Faraday Soc.*, **65**, 3258 (1969).
17) C. J. Marzzacco, G. Deckey, R. Colarulli, G. Siuzdak, and A. M. Halpern, *J. Phys. Chem.*, **93**, 2935 (1989).
18) J. D. Simon and K. S. Peters, *Acc. Chem. Res.*, **17**, 277 (1984).
19) A. K. Mishra, M. Sato, H. Hiratsuka, and H. Shizuka, *J. Chem. Soc., Faraday Trans.*, **87**, 1311 (1991).
20) T. Mabuchi and T. Fujii, in preparation.